Engineering Geology 195 (2015) 185–195

Contents lists available at ScienceDirect

Engineering Geology

journal homepage: www.elsevier.com/locate/enggeo

Discontinuity spacing analysis in rock masses using 3D point clouds

Adrián J. Riquelme [a,*], Antonio Abellán [b], Roberto Tomás [a]

[a] Departamento de Ingeniera Civil, Universidad de Alicante, Alicante, Spain
[b] Risk Analysis Group, Institut des sciences de la Terre (ISTE), Facult des Gosciences et de l'Environnement, Universit de Lausanne, Switzerland

ARTICLE INFO

Article history:
Received 18 August 2014
Received in revised form 5 May 2015
Accepted 14 June 2015
Available online 19 June 2015

Keywords:
Spacing
Discontinuity
3D point cloud
Rock mass
LiDAR 3D laser scanner

ABSTRACT

The complete characterization of rock masses implies the acquisition of information of both, the materials which compose the rock mass and the discontinuities which divide the outcrop. Recent advances in the use of remote sensing techniques – such as Light Detection and Ranging (LiDAR) – allow the accurate and dense acquisition of 3D information that can be used for the characterization of discontinuities.

This work presents a novel methodology which allows the calculation of the normal spacing of persistent and non-persistent discontinuity sets using 3D point cloud datasets considering the three dimensional relationships between clusters. This approach requires that the 3D dataset has been previously classified. This implies that discontinuity sets are previously extracted, every single point is labeled with its corresponding discontinuity set and every exposed planar surface is analytically calculated. Then, for each discontinuity set the method calculates the normal spacing between an exposed plane and its nearest one considering 3D space relationship. This link between planes is obtained calculating for every point its nearest point member of the same discontinuity set, which provides its nearest plane. This allows calculating the normal spacing for every plane. Finally, the normal spacing is calculated as the mean value of all the normal spacings for each discontinuity set.

The methodology is validated through three cases of study using synthetic data and 3D laser scanning datasets. The first case illustrates the fundamentals and the performance of the proposed methodology. The second and the third cases of study correspond to two rock slopes for which datasets were acquired using a 3D laser scanner. The second case study has shown that results obtained from the traditional and the proposed approaches are reasonably similar. Nevertheless, a discrepancy between both approaches has been found when the exposed planes members of a discontinuity set were hard to identify and when the planes pairing was difficult to establish during the fieldwork campaign. The third case study also has evidenced that when the number of identified exposed planes is high, the calculated normal spacing using the proposed approach is minor than those using the traditional approach.

1. Introduction

Rock mass, which can be defined as blocks of rock material separated by discontinuities, such as joints, faults, bedding planes, and so on (Bieniawski, 1989), is one of the most important concepts in rock engineering. The discontinuity properties (i.e., spacing, persistence, roughness, infilling, weathering and presence of water) have a capital importance on the geomechanical behavior of the rock mass (Bieniawski, 1973; Priest and Hudson, 1976), and are usually characterized through classical time-consuming techniques (e.g., compass which are commonly utilized in order to obtain discontinuity orientation and also conventional measuring tapes which are used for the estimation of discontinuity spacing; Palmstrom, 2001). Alternatively to manual discontinuity characterization, it is possible to use remote sensing techniques to acquire 3D information of the terrain with high accuracy and high spatial resolution (Jaboyedoff et al., 2012). The two most commonly employed remote sensing techniques for discontinuity analysis are Light Detection and Ranging (LiDAR) and digital photogrammetry.

Nowadays, LiDAR and digital photogrammetry techniques are widely accepted techniques for discontinuity analysis (Abellán et al., 2014; Jaboyedoff et al., 2012; Oppikofer et al., 2009; Viero et al., 2010). The number of publications has exponentially grown in the last years and has been able to successfully extract the orientation of discontinuities (Slob et al., 2005; Olariu et al., 2008; Sturzenegger and Stead, 2009b; Sturzenegger et al., 2011; Jaboyedoff et al., 2007; Garca-Sellés et al., 2011; Khoshelham et al., 2011; Gigli and Casagli, 2011; Lato and Vöge, 2012; Riquelme et al., 2014). Once discontinuities are identified and the 3D point cloud is classified, it is then possible to use this information to analyze spacing (Oppikofer et al., 2009; Slob, 2010), persistence (Sturzenegger and Stead, 2009a; Sturzenegger et al., 2011; Umili et al.,

* Corresponding author.
E-mail addresses: adririquelme@gmail.com, ariquelme@ua.es (A.J. Riquelme), antonio.abellanfernandez@unil.ch (A. Abellán), roberto.tomas@ua.es (R. Tomás).
URL's: http://personal.ua.es/en/ariquelme (A.J. Riquelme), http://www.3d-landslide.com (A. Abellán), http://personal.ua.es/en/roberto-tomas (R. Tomás).

http://dx.doi.org/10.1016/j.enggeo.2015.06.009
0013-7952/

2013) and roughness (Haneberg et al., 2007; Sturzenegger and Stead, 2009a; Oppikofer et al., 2011).

The aim of this paper is to present a new method for the calculation of discontinuity spacing from a rock mass using 3D point clouds. The main novelty of this method is that the proposed methodology allows computing the discontinuity spacing of persistent and non-persistent discontinuities, which are usually studied considering an infinite plane approach. The studied area must be representative of the rock mass properties and only those discontinuities that can reasonably be considered as planes should be studied, otherwise this method could lead to significant errors in the determination of the discontinuity spacing. The input of this method is a 3D point cloud, where each point has previously been classified by an assignment to a discontinuity set and to an aggregation of points belonging to the same discontinuity plane (hereinafter referred to as 'cluster'). Any reliable method that classifies the points and extracts their cluster planes can be applied. The approach used in this paper is the Discontinuity Set Extractor (DSE, available on http://personal.ua.es/en/ariquelme/), an open source software developed by Riquelme et al. (2014), which allows the user to calculate the cluster planes with the discontinuity set orientation or with the best fitting plane.

To summarize, the proposed methodology extracts rock mass discontinuities from rock masses affected by persistent and/or non-persistent discontinuity sets using 3D point clouds through the open source software DSE. Then, the relative location of the clusters on the space is analyzed and the spacing between the different discontinuities is calculated. Finally, the results obtained in three different case studies using the proposed method have been compared with those derived from field observations and discussed.

2. Previous considerations

Discontinuity spacing plays a key role in the behavior of the rock masses and has to be accurately computed. The ISRM considers the spacing as a descriptive index and recommends measuring it counting the number of discontinuities that cut a traverse line of known length (ISRM, 1977). However, new remote sensing techniques such as LiDAR allow performing a more realistic and accurate measurement of discontinuity spacing in three dimensions for each different discontinuity set.

2.1. Considerations on discontinuity spacings

Piteau (1970) proposed a widely used method to calculate the spacing between discontinuities. This author proposed the use of a scanline survey technique for the calculation of the discontinuity intensity. This parameter was defined as the number of discontinuities per unit distance, assuming a normal direction to the strike of a set of discontinuities (Priest and Hudson, 1976).

Originally, the ISRM defined the spacing between adjacent discontinuities as the distance between two correlative discontinuities which cut a traverse line of known length (ISRM, 1977). The ISRM recommends expressing it as a mean fracture spacing in meters or millimeters (as in core logging). More recently, Palmstrom (2001) stated that the discontinuity set spacing is the normal or minimum distance between individual discontinuities within a discontinuity set. He claimed that in the case of surface observations (traces), it is usual to use the average of spacing for these sets and that frequently, it is possible to find random discontinuities, which do not necessarily belong to any discontinuity joint set. This spacing has influence on the rock mass global behavior, and defines its block size for each discontinuity set.

Consequently, the three types of discontinuity spacings described above can be summarized as (Priest, 1993; Slob, 2010):

- Total spacing: distance between a pair of adjacent discontinuities measured along a specific line, e.g., a scanline.
- Set spacing: distance between subsequent discontinuities or average spacing between discontinuities from the same set.
- Normal set spacing: distance between a pair of adjacent discontinuities, from the same set, perpendicular to the average orientation in that set.

2.2. Existing approaches for the discontinuity spacing calculation

In practice, analysis of discontinuity spacing using digital information (e.g., digital photographs, orthophotos, and 3D point clouds) can be carried out from several approaches:

- Graphical analysis using scaled digital images. This method is quite similar to the fieldwork approach. It requires properly identifying, and accurately measuring, the orientation and frequency of visible discontinuity surfaces or traces in a rock slope.
- 2D approaches and profile sections (Oppikofer et al., 2011; Slob, 2010). This is a widely used approach in order to compute discontinuity spacing using point clouds. Its main drawback is that results strongly depend on the chosen profile or virtual scanline.
- Fracture estimation analyzing two-dimensional fracture trace information gathered from digital images of exposed rockfaces (Kemeny and Post, 2003).
- Spacing analysis using 3D spatial relations. Normal spacing is calculated as the minimum distance (i.e., orthogonal distance) between exposed planes, measured in a perpendicular direction to one of those planes. If the two planes are not parallel, the distance depends on the location of the measuring line, but if they are parallel, it is a non-directional dependent method. This is the approach considered in this work to compute discontinuity spacing.

2.3. Cluster orientation

The rock outcrops members of a discontinuity set are usually not perfectly parallel due to natural structure complexity and to uncertainties of technique.

The normal procedure for measuring discontinuity spacing consists on intersecting both discontinuities by an arbitrary line. Then, the intersection of this line with the two planes defines two points, and the spacing will be equal to the distance between these two points. Although the orientation and spatial location of this line plays a capital role on the calculation of the discontinuity spacing, there is no common agreement on the parametrization of this variable. For instance, some authors define the direction of this line as parallel to the normal vector of the discontinuity set, nevertheless the spacing values are still affected by the arbitrary selection of the line location (Slob, 2010). This problem can be fixed considering that all clusters have the same orientation of the principal plane of the given discontinuity set, which is a reasonable assumption when the discontinuities are parallel within the studied region. Therefore, in this approach it is required that the normal vector of each cluster plane is equal to the normal vector of the discontinuity set.

3. Methodology: the 3D spacing approach

3.1. Input data

Every point of the point cloud has to be previously assigned to a discontinuity set and to a given cluster (see Appendix A). The necessary inputs for every point are:

- (X, Y, Z) coordinates
- Discontinuity set id
- Cluster id
- Normal vector of the discontinuity set (A, B, C) (Eq. (1))

- Normal vector of the cluster (A, B, C) (Eq. (1))
- Plane position of the cluster: parameter D (Eq. (1))

where the plane equation is written as:

$$A \cdot x + B \cdot y + C \cdot z + D = 0. \quad (1)$$

3.2. 3D discontinuity spacing calculation

The normal spacing is the distance between discontinuity planes measured along an orthogonal scanline (Palmstrom, 2001), but this definition is not easy to apply when the data are discontinuity planar outcrops unlinked and distributed in the 3D space (point cloud clusters). In this case, these planes may not be intersected by an orthogonal scanline and thus it is needed to make some hypothesis to apply the previous definition.

Unlike existing methods which presume full persistence (e.g., Slob, 2010), non-persistent discontinuities are considered in our methodology. This assumption adds an additional complexity to the discontinuity spacing calculation. A key point of our approach is the fact that the link between clusters is defined considering the three dimensional relationships between clusters, calculating the spacing by measuring the orthogonal distance between a given cluster and its nearest neighbor cluster. A graphical clarification of this concept is given in Fig. 1, where in order to provide a simpler and more comprehensive explanation, the discontinuities have been represented in 2D. This figure shows an orthogonal cross-section of the point cloud containing six different clusters and the different approaches used for calculating their normal set discontinuity spacing: full persistent and non-persistent procedures. When considering non-persistent discontinuities (Fig. 1b), cluster 3 is the closest feature to cluster 1. Nevertheless, when considering full persistent discontinuities (Fig. 1a), cluster 2 is the closest feature to cluster 1. Then, the calculation of the discontinuity spacing for each cluster generates a completely different distribution of discontinuity spacing: considering full persistence the mean normal spacing results in 16.28 units and considering non-persistent discontinuities the mean normal spacing results in 27.16 units. These results show close resemblance to the ones using standard geomechanical stations, where measurements are taken between close discontinuity surfaces or traces. The main advantage in this case is that calculation is carried out in an automatic 3D point clouds.

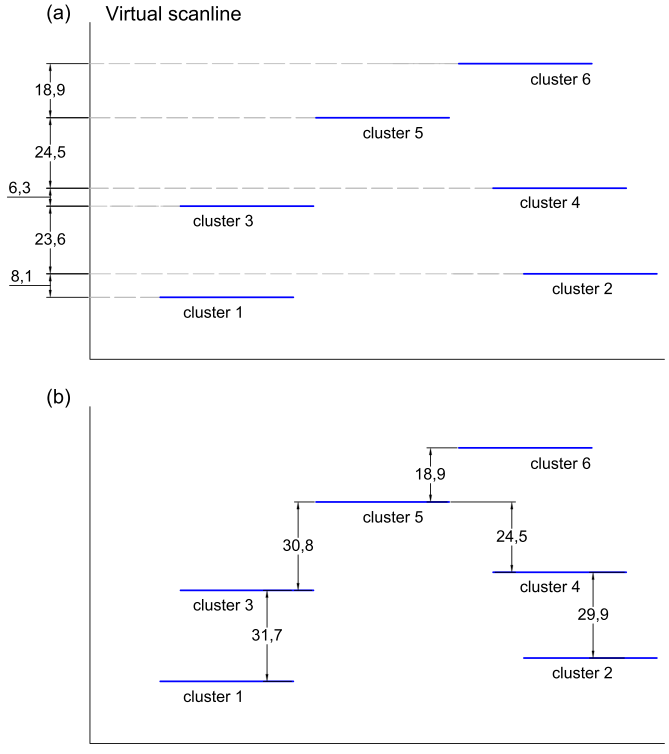

Fig. 1. Scheme of the cluster linking and the discontinuity normal set spacing considering (a) full persistence and (b) non-persistence of the discontinuities. Blue thick lines represent the discontinuities.

Therefore, for calculating the distance between clusters we operate as follows: firstly, all the cluster planes are sorted in ascending order by using the D parameter, giving as a result the list *Dsorted*. Then, the algorithm creates the point set R, which includes all the points of the discontinuity set omitting the points contained on the first cluster. For each point of this cluster, the algorithm searches for the nearest neighbor point within the dataset R. The closest point is member of its closest cluster, and thus, its corresponding distance is the spacing between these two clusters. The algorithm continues with the corresponding following cluster in the list *Dsorted*. The points of this cluster are excluded from the R dataset in order not to repeat spacing calculations. The process continues until all the clusters are computed. At the end, a list of spacing values is provided, including the cluster identifiers used for this calculation.

Algorithm 1. Calculation of the normal spacing using 3D point clouds.

```
procedure SPACING CALCULATION
    Input: Point Cloud P=(X, Y, Z, DS id, cl id, A, B, C, D)
    Output: Spacing = (DS id, cl1 id, cl2 id, spacing, cl1 D, cl2 D)
    counter = 1
    for each joint set i do
        P_i ← P                                   ▷ P: points member of DS id i
        P_i ← Sort P_i by D parameter             ▷ in ascending order
        Dsorted ← D values of all the points of P_i
        Dsortedid ← cluster ids of all the points of P_i
        create group R ≡ P(points members of P_i except cluster id Dsortedid(1))
        for each cluster j do
            create group Q ≡ P_i(points members of P_i and cluster id Dsortedid(j))
            Dist ← Distance from all the points of Q to all the points of R
            p ← nearest point from Q to R
            pid ← id of the cluster that contains the point p
            D_1 ← D parameter of the cluster that contains the cluster id Dsortedid(j)
            D_2 ← D parameter of the cluster id pid
            spacing(counter) ← [DS i, cl Dsortedid(j), pid, |D1 − D2|, D_1, D_2]
            create group R ≡ R(points members of R except cluster id Dsortedid(i))
            counter ← counter + 1
```

3.3. Statistical analysis

The statistical analysis calculates the non-parametric distribution by means of the *kernel density estimation* technique (Silverman, 1986). The normal spacing is calculated as the mean of the calculated distances. Moreover, in this work the following population statistics are calculated: min, max, mode, mean, maximum density value and standard deviation.

4. Case studies

In this section, the above described method is applied to three different cases of study. The first one corresponds to a synthetic case in which a regular table is modeled. In the second and third case studies, the discontinuity spacings of two rock slopes are analyzed using 3D data acquired by means of a 3D laser scanner. Case study 1 focuses on how the spacing is calculated, illustrating the establishment of the connections between clusters. Case studies 2 and 3 correspond to real rock mass surfaces, and their aim is to demonstrate the reliability of the proposed method to calculate discontinuity spacings of rock slopes through 3D point cloud data acquired by terrestrial remote imaging techniques.

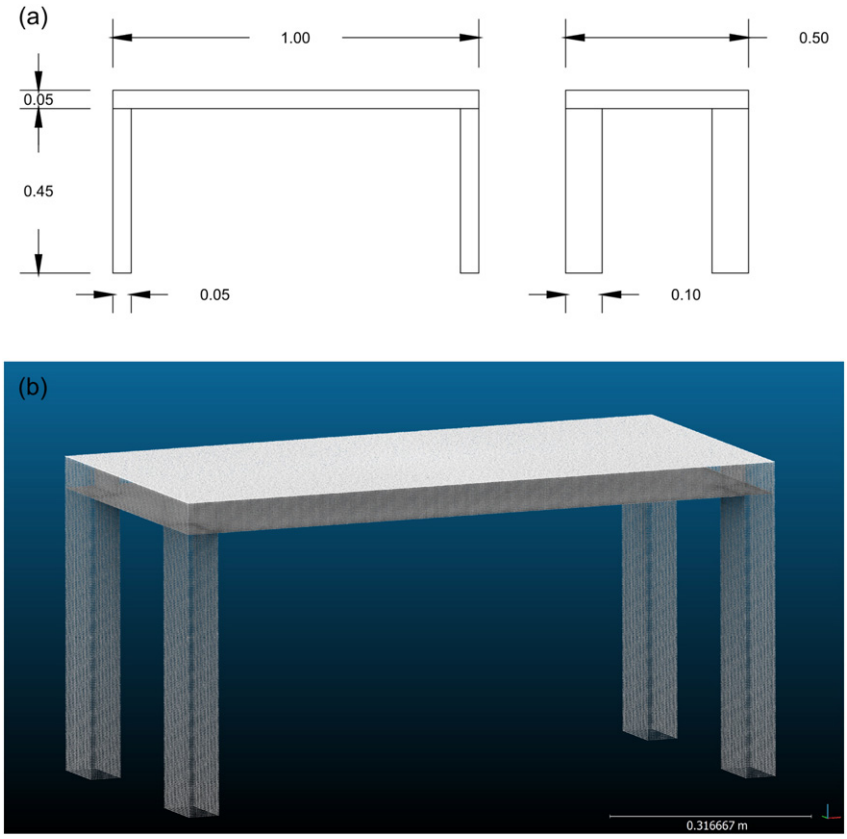

Fig. 2. Case study 1. (a) Map of the studied table, dimensions are in meters; (b) Synthetic point cloud of the table, where all sides of the table are orthogonal.

4.1. Case study num. 1: dining table (synthetic point cloud)

This case study analyzes a very simple geometry: a small dining room table shown in Fig. 2a and b. In this case the 3D point cloud was generated by means of a simple MATLAB code (MATLAB, 2013).

4.2. Case study num. 2: rock slope I (El Campello, Spain)

This case of study analyzes a rock slope excavated in limestones located in El Campello (SE Spain). The approximate size of the analyzed area is 7.5 × 2.5 m (Fig. 3). The 3D dataset was acquired by a laser scanner survey developed on January 12th, 2015 with a Leica C10 laser scanner. In order to reduce shadow areas, the data acquisition was performed in three separate stations using planar targets as reference points and the point cloud was registered using data from a digital map (SIGNA http://signa.ign.es/signa/). The studied sector was subsampled obtaining a point cloud with 26884 points (a point density of 1250 pts/m^2).

4.3. Case study num. 3: real rock slope II (City of Alicante, Spain)

In this case study an urban rock slope excavated in marly limestones in the City of Alicante (SE Spain) is analyzed. This rock mass presents some practical difficulties for its characterization for four reasons:

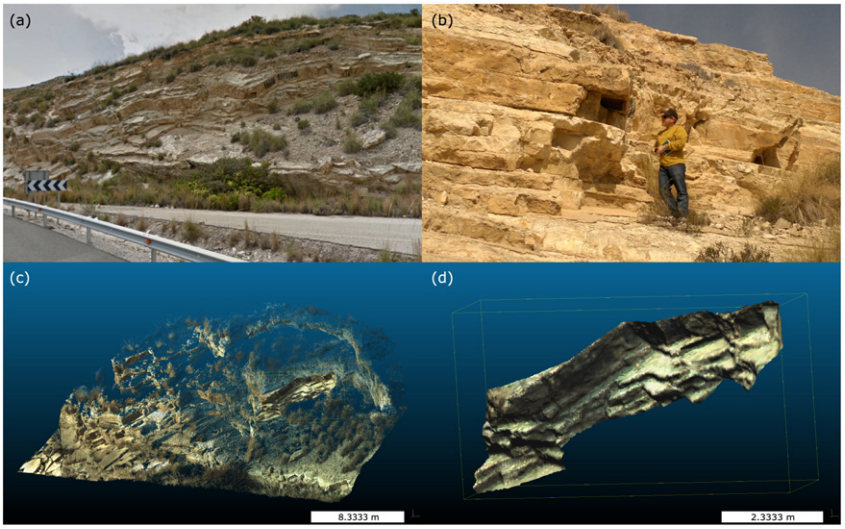

Fig. 3. Case study 2: rock slope in El Campello, SE Spain. (a) Picture of the site; (b) Picture of the fieldwork campaign; (c) 3D point cloud acquired with 3D laser scanner; (d) Analyzed sector.

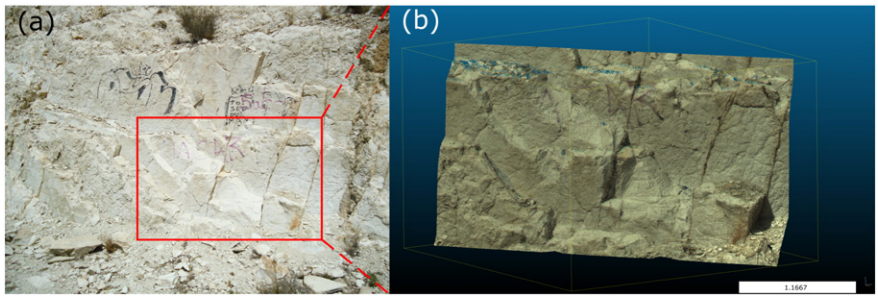

Fig. 4. Case study 3: urban rock slope in the City of Alicante. (a) Picture of the site; (b) 3D point cloud of the slope.

(a) most of the discontinuity surfaces are smoothed by weathering; (b) the strata is slightly folded and eventually affected by several normal faults; (c) In addition, the sub-horizontal surfaces are partially (or even completely) covered by debris due to the progressive degradation of the materials located at the upper part of the slope; and (d) some of the discontinuity sets are not persistent. Consequently, a representative outcrop of the rock mass has been selected to minimize these mentioned effects that can mask the true discontinuity surfaces. The approximate size of the analyzed area is 3×2 m (Fig. 4). The 3D dataset was acquired by a laser scanning survey carried out on March 28th, 2015 with a Leica C10 laser scanner. In order to reduce shadow areas, the data acquisition was performed in three separate stations using planar targets as reference points and the point cloud was registered using data from a digital map (SIGNA http://signa.ign.es/signa/). The studied sector was subsampled obtaining a point cloud with 301089 points (a point density of 8×10^4 pts/m^2).

5. Results

5.1. Case study num. 1

The surface of the studied solid is defined by three orthogonal planes, and thus three orthogonal discontinuity sets are expected to be found: J_1 that refers to the horizontal surfaces of the table and J_2

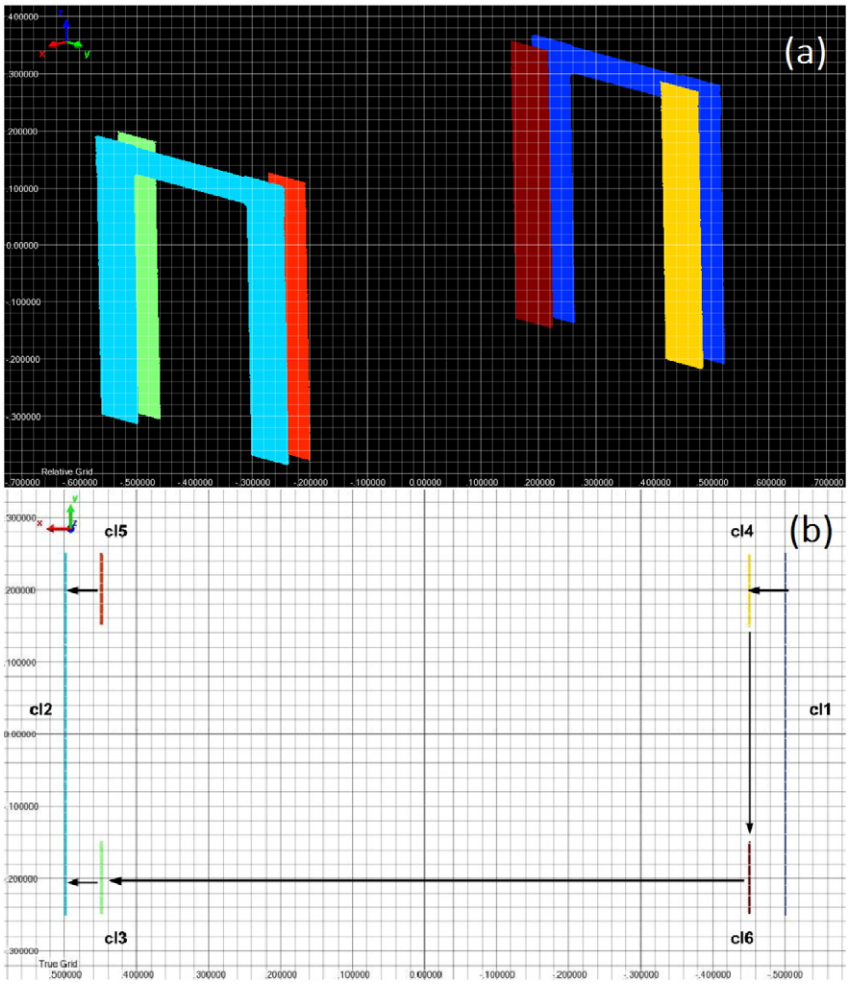

Fig. 5. Case study 1, results (I): (a) Discontinuity set 2 depiction. Six clusters (cl) are depicted, cl1 in blue, cl2 in cyan, cl3 in green, cl4 in yellow, cl5 in orange and cl6 in brown. (b) Top view of the table. Note that in order to calculate the spacing the relations between clusters are indicated using black arrows.

Table 1
Case study 1, results (I): synthetic table. Cluster relation analysis and spacing calculations, discontinuity set J_2.

DS	Cl_i	Cl_j	D_i [m]	D_j [m]	$\lvert D_i - D_j \rvert$ [m]	Real distance [m]	Abs error [m]	Relative error [%]
2	1	4	−0.4927	−0.4485	0.0442	0.05	0.0058	12
2	4	6	−0.4485	−0.4392	0.0093	0.00	0.0093	–
2	6	3	−0.4392	0.4603	0.8995	0.90	0.0005	0
2	5	2	0.4510	0.5068	0.0558	0.05	0.0058	12
2	3	2	0.4603	0.5068	0.0465	0.05	0.0035	7

and J_3 which refer to the vertical planes. The analysis shows three principal orientations, corresponding to the different sides of the table: four rectangular legs and the table top. This example aims showing how the spacing is calculated. We focus our attention specifically on J_2.

Fig. 5a shows the members of the clusters of the joint set 2 (J_2). The most repeated spacing should be 5 cm (Fig. 2) and a single value of 0.9 m should be found. The calculation process and the obtained results are, respectively, shown in Table 1 and Fig. 5. The first cluster used in order to calculate the spacing is the right one (cluster 1 in blue) whose plane equation shows the lowest D value. Once this cluster has been selected, the method searches for the following nearest cluster (cluster 4 in yellow), and calculates the distance between the cluster planes. The method continues with the following clusters sorted according to the D parameter dimension in ascending order (see Table 1). The calculated distances and the real distances between clusters are summarized in Table 1 in which absolute and relative errors in the determination of the spacing are also included.

5.2. Case study num. 2

The 3D point cloud processed in Fig. 3 has been processed to extract the identified discontinuity sets (see Fig. 6a). Six main orientations were obtained, where J_1 corresponds to the bedding plane and J_2, J_3, J_4, J_5 and J_6 are subvertical joints. Fig. 6c shows the classified point cloud using 3D dataset, where each discontinuity set is colored. The studied sector was analyzed using fieldwork data and four discontinuity sets were obtained (see Fig. 6b), where J_1 corresponds to the bedding plane and J_2, J_3 and J_4 are the subvertical joints. The comparison of both results shows that J_1, J_2 and J_4 have been identified by both approaches. Concerning the

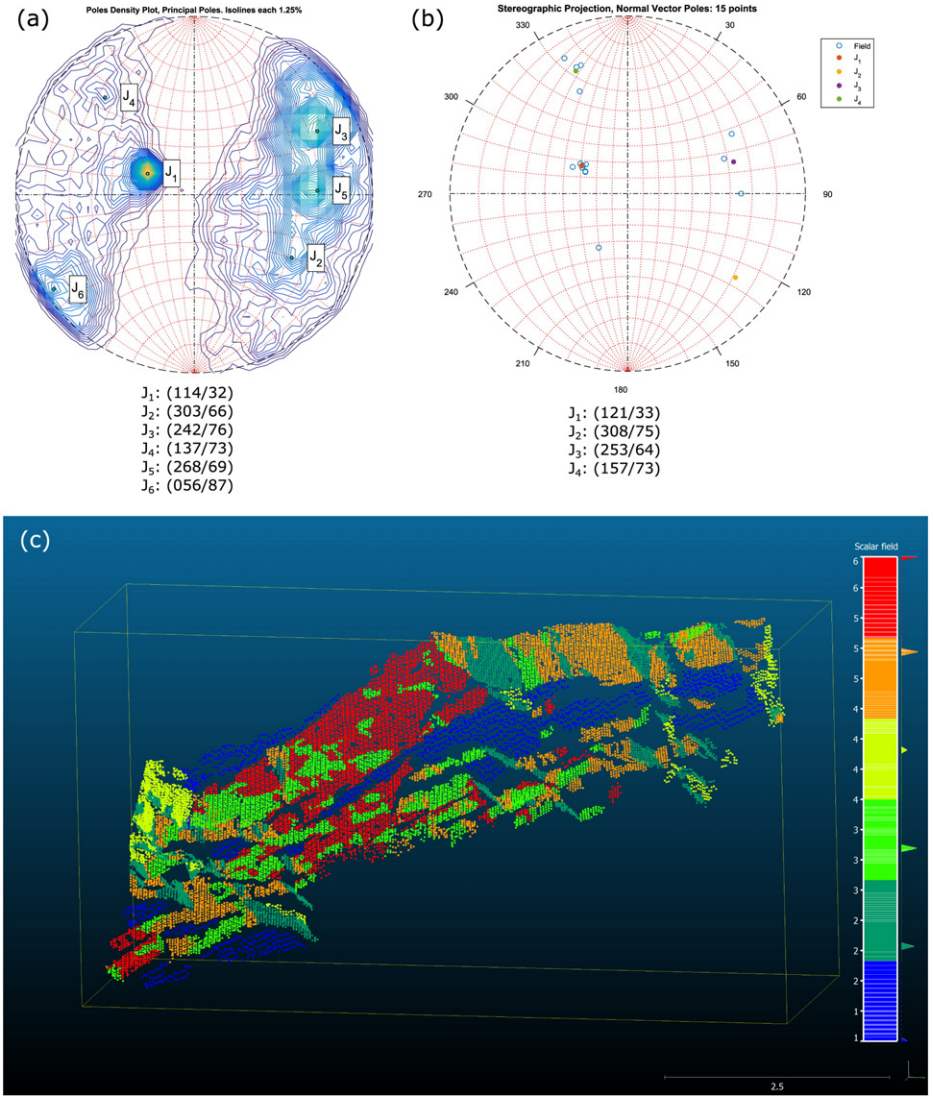

Fig. 6. Case study 1, results (I): El Campello, Alicante. Discontinuity set analysis for case study 2. (a) Results using 3D dataset; (b) Results from fieldwork; (c) Classified point cloud.

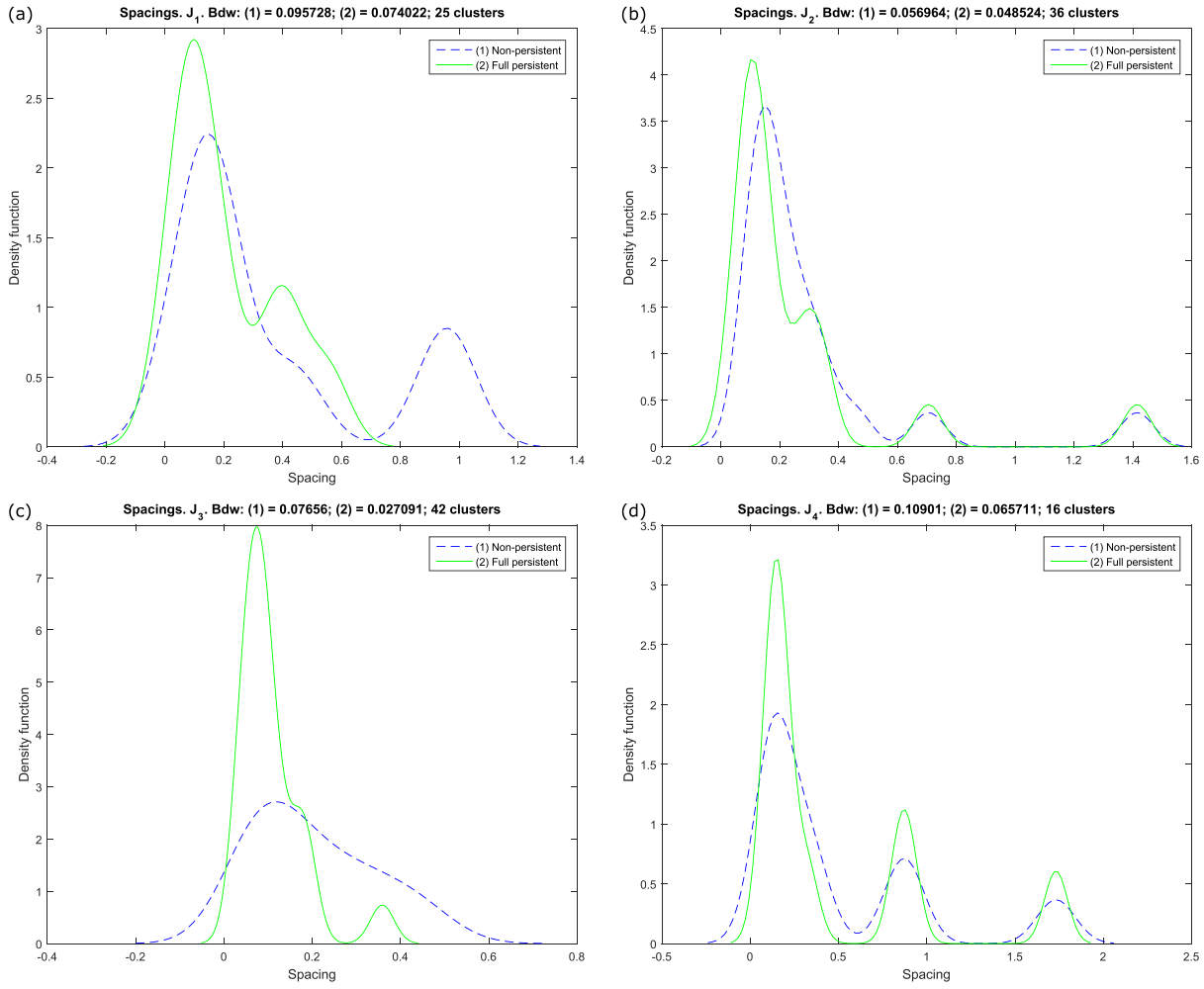

Fig. 7. Case study 2, results (II): El Campello, Alicante. Statistical analysis of the spacings for case study 3. Non-parametric density function of the spacing values: (a) J_1, (b) J_2, (c) J_3 and (d) J_4.

discontinuity set identified as J_3 using fieldwork data, Fig. 6b shows that it was extracted as a single discontinuity. Contrary the 3D analysis showed that previous DS was not identified as a single DS. Actually there were two discontinuity sets with statistic difference, but with similar dip direction and dip. Moreover, the 3D analysis extracted J_6, but the visual inspection showed that actually this discontinuity set corresponds to the conjugated plane of J_3.

The normal spacing was computed for each discontinuity set and results are summarized in Fig. 7 and Table 2.

Table 2
Case study 2, results (III): El Campello, Alicante. Statistic values of the spacing values. Comparison between persistent and non-persistent discontinuities.

	J_1		J_2		J_3		J_4	
	[m]	[m]	[m]	[m]	[m]	[m]	[m]	[m]
Persistence	No	Yes	No	Yes	No	Yes	No	Yes
Min	0.011	0.011	0.103	0.046	0.029	0.029	0.087	0.087
Max	0.988	0.553	1.415	1.415	0.490	0.359	1.732	1.732
Max dens	0.147	0.098	0.149	0.102	0.116	0.072	0.155	0.158
Mode	0.011	0.011	0.103	0.046	0.029	0.029	0.087	0.087
μ	0.355	0.206	0.296	0.259	0.202	0.107	0.484	0.469
σ	0.348	0.179	0.309	0.329	0.135	0.075	0.528	0.534
n clusters	59		39		57		35	
Field value	0.247		1.425		1.000		0.650	

5.3. Case study num. 3

The 3D point cloud shown in Fig. 4b has been processed in order to extract the discontinuity sets (Fig. 8a) and to classify the point cloud (Fig. 8b).

This analysis shows that discontinuity sets J_1, J_2, J_3 and J_4 are successfully identified (Fig. 8b to f). J_1 is the bedding plane and its exposed planes are defined by the calculated clusters (see Fig. 8c). J_2 is a sub-horizontal plane which is partially covered by debris (see Fig. 8d). J_3 is a sub-vertical plane which is easily identified by its corresponding traces on the slope surface and its outcropping planes (see Fig. 8e). J_4 is a discontinuity poorly represented in the slope that has been identified as their outcropping planes were statistically significant (see Fig. 8f).

The non-parametric density functions for each discontinuity set are shown in Fig. 9a, b, c and d and summarized in Table 3. As in previous case studies, spacing values considering the full persistence hypothesis are smaller than the ones obtained considering non-persistence hypothesis of the discontinuities. The field-measured discontinuity spacings were obtained by identifying the discontinuity traces and exposed planes which outcrop in the rock mass surface. Field values of the spacing were acquired measuring the normal spacing of visible and accessible exposed planes. This sampling method was applied to the bottom of the slope due to the difficult and unsafe access to higher areas. These values were calculated as the number of traces per meter, and then a correction (Terzaghi, 1965) was applied considering the

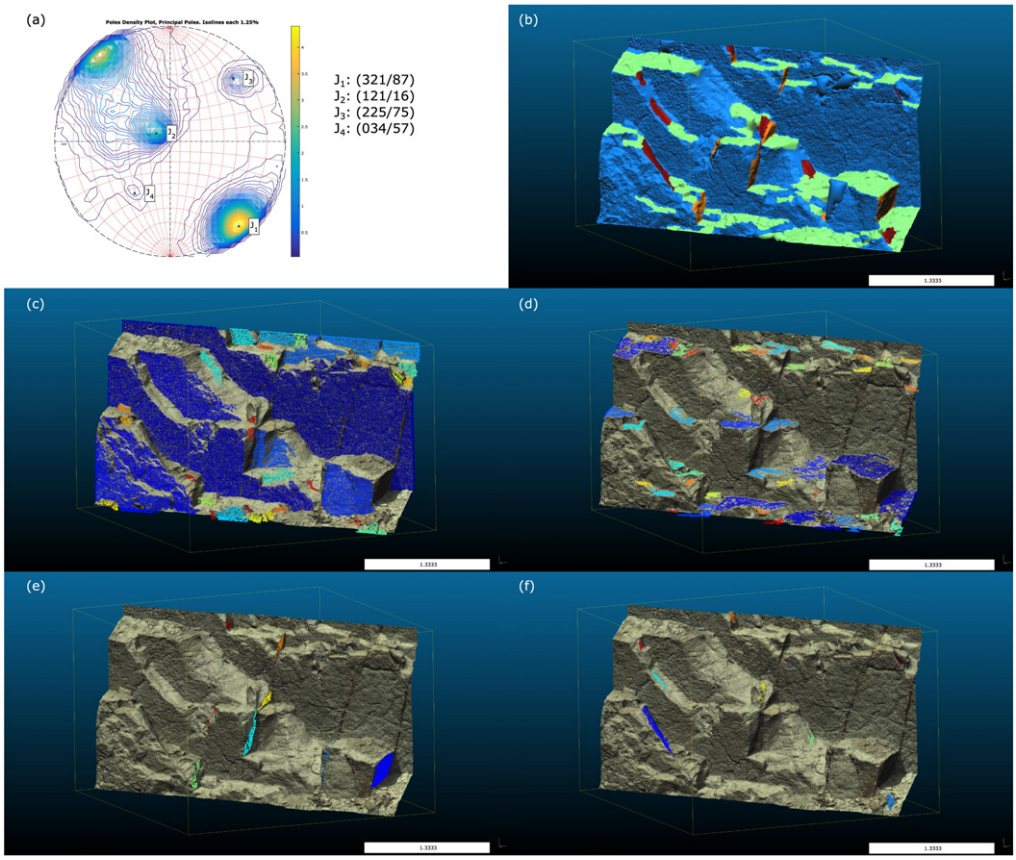

Fig. 8. Case study 3, results (I): City of Alicante. Statistical analysis of the planes. (a) Statistic analysis of the planes; (b) Discontinuity sets: J_1 points are in blue, J_2 are in green, J_3 are in orange and J_4 are in brown; (c) Clusters of discontinuity set J_1; (d) Clusters of J_2; (e) Clusters of J_3; (f) Clusters of J_4.

orientation of the surface and the discontinuity set orientation. Finally, the field value of the spacing was calculated as the mean of all the spacings within a set.

6. Discussion

The proposed method in this work has been proven useful in order to calculate discontinuity spacings and to identify cluster relations. Our approach is based on the three coordinates of surface points and no additional attributes (e.g., reflectance and color) are considered. This fact implies that traces on the rock surface are not taken into account, despite being a very useful information considered by other authors in order to calculate spacing (Kemeny and Post, 2003). The proposed methodology could be improved by considering information extracted from the discontinuity traces. Furthermore, the fact that discontinuities are considered as non-persistent implies that computed spacing values are higher or equal to those calculated with the full persistence hypothesis.

The method was tested using two different sources of information (synthetic data and 3D datasets using terrestrial LiDAR scans) showing a good adaptability. The first case study used synthetic data and allowed us to explain the relations between clusters and how spacing is calculated. In this case of study, due to the geometry of the example, both, the persistent and non-persistent approaches have to provide a similar normal spacing, as confirmed by the calculated mean absolute differences between the real and the calculated normal spacings (5 mm) and the mean relative difference (7.8%).

The second case study shows the algorithm application to a 3D point cloud dataset acquired by means of 3D laser scanner. Four discontinuity sets were extracted and normal spacings were calculated considering full persistence and non-persistence hypothesis. Then the results obtained through the traditional method and the proposed approach were compared. The results obtained through the proposed approach showed that the discontinuity sets J_1 and J_4 had the same order of magnitude than those obtained with the traditional approach. Contrary, it was observed that the normal spacings obtained using 3D point clouds were significantly minor than those obtained using the traditional method for J_2 and J_3. This inconsistency may be due to the fieldwork acquisition process and to the particular field conditions. A possible explanation for this result is that: (1) these two discontinuity sets were identified by their exposed planes and not by their traces; and that (2) the exposed planes were not clearly linked at field and thus the minimum distance between them was not accurately measured. Due to this fact, fieldwork spacing data acquisition required: (1) first the identification of those surfaces that belonged to the identified discontinuity set; (2) the visual identification of how each exposed plane is linked to the nearest one; and (3) the normal spacing measurement between paired exposed planes. This process can be really hard if exposed planes are not clearly mappable and if discontinuity sets have close orientations. Contrary, the use of 3D datasets allowed the analytical definition of exposed planes and no physical restriction conditioned the spacing measurements. This is the reason why when using 3D point clouds, more clusters were detected than when using the traditional approach. Moreover, this effect had an influence on the minor resulting normal spacing. This finding suggest that the use of 3D point clouds may lead to different normal spacing values than those obtained using the traditional approach when outcrop conditions difficult the data acquisition.

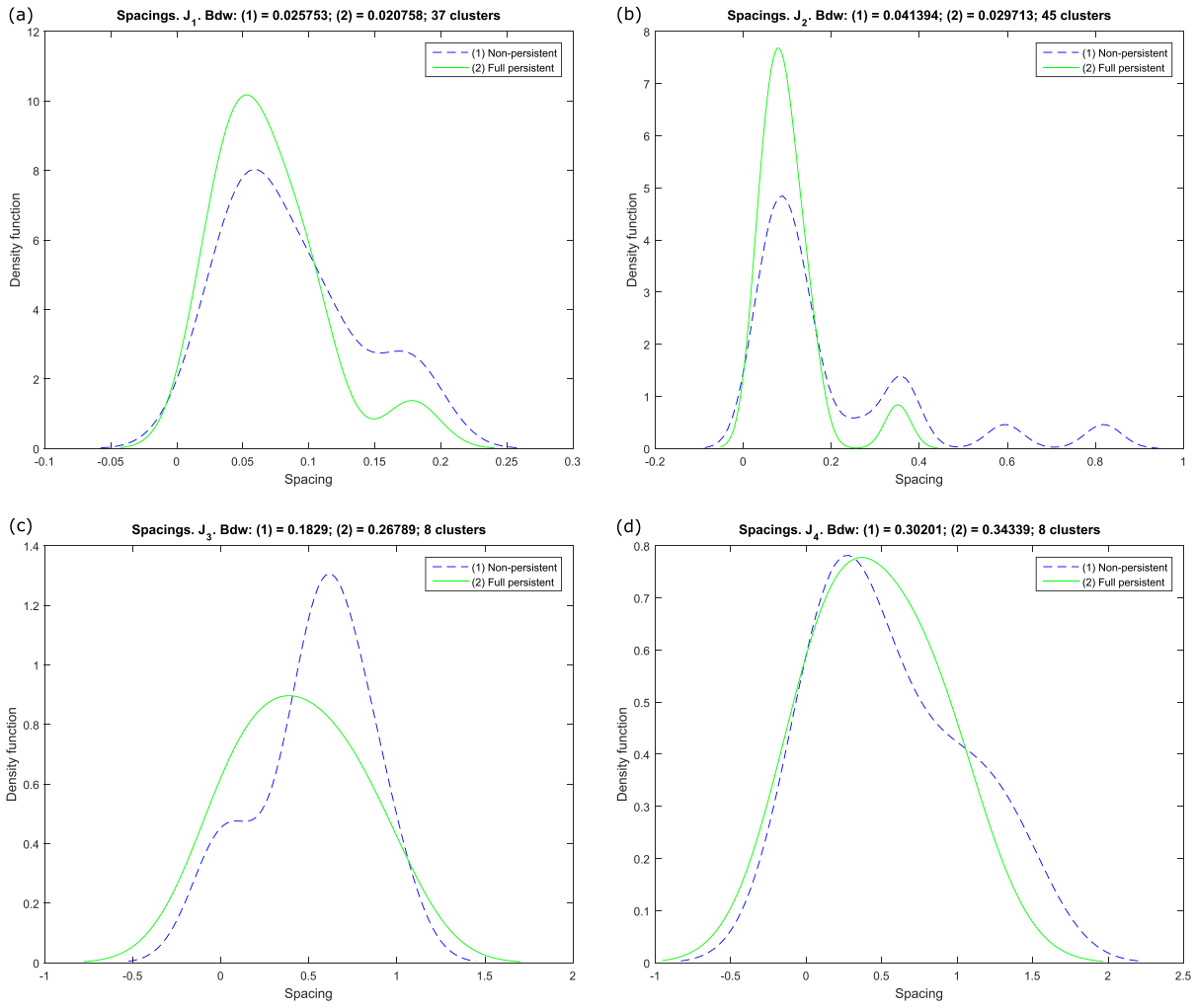

Fig. 9. Case study 3, results (II): City of Alicante. Statistical analysis of the spacings. Non-parametric density function of the spacing values: (a) J_1, (b) J_2, (c) J_3 and (d) J_4.

The third case study (rock slope in the City of Alicante, Spain) is a 3D laser scanner dataset of an urban rock slope. The current results pointed that the calculated normal spacings reasonably matched the field measurements values. Nevertheless, the results derived from 3D point clouds are minor than those obtained using the traditional approach when the number of extracted clusters is high. A possible explanation for this fact is that during fieldwork several small clusters were not identified, were considered as random isolated discontinuities or were inaccessible. Thus, the analysis using 3D point clouds provided more clusters within the same area, and computed discontinuity spacings were minor. On the other hand, an experienced engineer would be able to identify clusters of a discontinuity set and also to discard non-valid values, while DSE software would consider all exposed planes with the same orientation. As a result, we can conclude that this method has to be used with a proper background in rock mechanics.

Table 3
Case study 3, results (III): City of Alicante. Statistic values of the spacing values. Comparison between persistent and non-persistent.

	J_1		J_2		J_3		J_4	
	[m]	[m]	[m]	[m]	[m]	[m]	[m]	[m]
Persistence	No	Yes	No	Yes	No	Yes	No	Yes
Min	0.020	0.020	0.037	0.037	0.024	0.024	0.075	0.075
Max	0.181	0.178	0.818	0.351	0.900	0.900	1.327	0.935
Max dens	0.057	0.052	0.09	0.077	0.611	0.399	0.284	0.372
Mode	0.020	0.020	0.037	0.037	0.024	0.024	0.075	0.075
μ	0.086	0.069	0.196	0.103	0.529	0.437	0.554	0.453
σ	0.051	0.042	0.202	0.075	0.323	0.344	0.488	0.361
n clusters	37		45		8		8	
Field value	0.172		0.224		0.397		0.503	

One of the strengths of the presented method consists on using the original information contained in 3D points during all the process, and considering discontinuities as non-persistent instead of considering all clusters as infinite planes. Therefore, obtained results considering the non-persistence of discontinuities are equal or higher than the ones obtained considering full persistence. Although the method only uses the geometric information of the surface, there is still a very valuable information to be considered, such as discontinuity traces from the rock mass surface. In addition to this, although a great improvement in workflow automation is obtained using the proposed approach, a solid background in rock mechanics together with fieldwork recognition is required for an optimum application of the proposed method.

Further research lines point out to a continuous software development in order to obtain geomechanical parameters (e.g., persistence and roughness) from the scanned rock masses; furthermore, we support the development of a more reproducible research thanks to new trends in code and data sharing under GNU GPL license (e.g., www.reproducibleresearch.net). In order to contribute to the latter, the

complete 3D RAW and processed datasets will be freely available in our website (www.3D-landslide.com/spacing).

7. Conclusions

A new method for calculation of discontinuity set spacings from 3D point cloud data has been presented. This method is based on the classical definition of the spacing, but instead of using a single virtual scanline our method uses the relative positions of clusters to establish how they are linked.

First, this paper considers the existing previous ways to calculate spacings, and focuses specifically on those that use 3D point clouds. After the analysis, some weaknesses of these methods are detected and some solutions are proposed to fix them.

The input of the proposed method consists on a 3D point cloud data, where each point is classified in relation to a discontinuity set and is assigned to a cluster of points belonging to a given discontinuity set. Each cluster is fitted to a plane parallel to the main orientation of its discontinuity set and thus, all clusters members of a discontinuity set are parallel. First, for each discontinuity set all clusters are sorted in ascending order according to the cluster plane D parameter. Following this sorted cluster identifiers array, the closest cluster is determined for each cluster, and the normal spacing is calculated as the normal distance between them. The used cluster is then removed from the database in order to avoid repeated links in following calculations. Consequently, as all cluster planes are extracted parallel to their discontinuity set, spacing is calculated as the distance between two linked clusters. As a result, spacing is calculated considering the non-persistence of discontinuities, which increases the reliability of the method.

This developed approach, which can be used to estimate discontinuity spacing in inaccessible or dangerous outcrops, will help programming the 3D calculation of the degree of fracturing on rock slopes. This will help rock mass scientists and practitioners obtaining more accurate and more reproducible rock mass quality assessment and block size distribution for quarrying. In addition to this, the proposed approach considers the non-persistence of discontinuities, and allows the possibility of considering persistence values for further researches.

Acknowledgments

This work was partially funded by the Swiss National Science Foundation (FNS-138015 and FNS-144040 Projects), the Spanish Ministry of Economy and Competitiveness (MINECO) and EU FEDER under Projects TEC2011-28201-C02-02 and TIN2014-55413-C2-2-P, the Spanish Ministry of Education, Culture and Sport in the framework of the Programa Estatal de Promocin del Talento y su Empleabilidad en I + D + i under project PRX14/00100 and by the Generalitat Valenciana under Project ACOMP/2014/136. The authors would like to acknowledge Prof. Didier Hantz for his stimulating discussion at an early stage of this manuscript concerning the calculation of discontinuity spacing. Special thanks are also due to the computers provided by Mrs. Angela Prats and Mr. Javier Soler, which have considerably speeded up our computation time. Finally, we would like to acknowledge Mrs. Esther Coves and Mr. Vincent Alcala for the English language revision and correction of this manuscript. Their help is kindly appreciated.

Appendix A. Cluster alignment

One of the discontinuity spacing analysis issues is that discontinuities are commonly non-persistent planes, except for the bedding planes in sedimentary rocks, where they are usually full persistent. Discontinuities are usually characterized at field from outcrops or traces. Then, if a discontinuity crops out in different positions from the rock mass, it becomes hard to determine if they belong to the same discontinuity (and therefore to a given plane) or not. From an analytical perspective, two set of points of the same discontinuity set will have the same normal vector (A, B, C), and a different plane position value D (Eq. (1)). It is unlikely that the two clusters from the same discontinuity set present exactly the same D value, but they will have similar values and thus can be erroneously interpreted as different discontinuity planes.

In order to solve this ambiguity, a simple approach is proposed to state when two clusters belong to the same plane. Let's consider a cluster a that belongs to the discontinuity set i. The points of the cluster are distributed around its cluster plane. It is possible to calculate the distance of all the points' members of a cluster to its plane, obtaining a density function with mean μ_a and standard deviation σ_a. Furthermore, let's consider another cluster b, candidate to belong to the same discontinuity than the cluster a, with a mean μ_b and a standard deviation σ_b. When both sets of points from the clusters a and b are different parts of the same plane, then these two clusters will be so close that there will be an important overlap of their respective density functions which will be higher than a certain threshold value.

Since each 3D point dataset has its own precision, the proposed test considers the dispersion of the points by means of the standard deviation σ. Firstly, the mean μ and the standard deviation σ of each distance distribution are calculated. Secondly, the segment centered in μ that have lengths 2 k times the standard deviation σ for each distribution is computed, where k is a positive number (Appendix Fig. A.1a). Then, if the segments $\mu \pm k \cdot \sigma$ of both distributions intersect, it is reasonable to consider them as members of the same plane, and thus, no spacing will be calculated between those two clusters (Appendix Fig. A.1b). Otherwise, both distributions will be considered to belong to different planes and the spacing will be subsequently calculated if it is needed (Appendix Fig. A.1c).

It can be stated that two point clouds, members of planar surfaces with the same orientation (i.e., the same A, B and C parameters) and with D_a and D_b parameters respectively belong to the same plane when:

$$k \cdot (\sigma_a + \sigma_b) \geq |D_a - D_b| \tag{A.1}$$

where:

σ_a is the standard deviation of the cluster a;
σ_b is the standard deviation of the cluster b;
D_a is the location parameter (Eq. (1)) of the cluster plane a, equal to μ_a;
D_b is the location parameter (Eq. (1)) of the cluster plane b, equal to μ_b; and
k is the parameter which controls how close the two distributions must be to be considered as the same cluster.

Eq. (A.1) evaluates the intersection of the two density functions (i.e., the overlap between the sigma lines of both considered density functions in terms of σ; Appendix Fig. A.1a). Low k values indicates that a high overlap between both density functions is needed in order to consider that the two clusters have the same position in the space (i.e., they are the same plane). The value of $k \cdot \sigma$ depends on the accuracy of the point cloud, but experience shows that values of $k = 1$ usually offer reasonable results.

Finally, if this test establishes that two clusters belong to the same discontinuity, the parameter D_b of the cluster b is then redefined as equal to the value of the parameter D_a. In other words, at this step we perform an adjustment of the position of the plane.

This adjustment should be applied for planar discontinuities. When the clusters are too big or very wavy, the standard deviation and the length of the segment $2k\sigma$ are very high. Therefore, different clusters could be considered members of the same discontinuity. Additionally, if spacing between discontinuities is of the same level of magnitude than the instrumental error this adjustment should not be applied, i.e., in foliated rock masses when using standard terrestrial LiDAR.

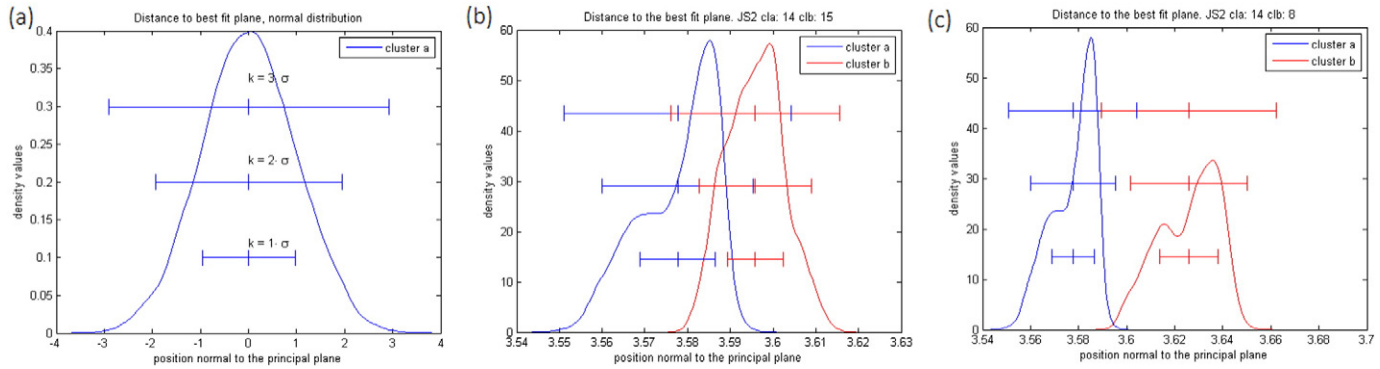

Appendix Fig. A.1. Density functions of the distance point to the best fit plane: (a) Normal distribution of points to plane distance, where the first segment lengths two sigmas, the second four sigmas and the third six sigmas; (b) Two clusters very close, two sigma lines overlap; (c) Two separated clusters, only three sigma lines overlap. The three horizontal lines are centered in the mean value of each distribution. Each line lengths $2 \cdot k \cdot \sigma$ ($k = 1$ bottom, $k = 2$ middle, $k = 3$ upper). Note that the lines overlap depending on how close are the center of the distribution (μ) and the dispersion of the points (σ).

References

Abellán, A., Oppikofer, T., Jaboyedoff, M., Rosser, N.J., Lim, M., Lato, M.J., 2014. Terrestrial laser scanning of rock slope instabilities. Earth Surf. Process. Landf. 39, 80–97.

Bieniawski, Z., 1973. Engineering classification of jointed rock masses. Civ. Eng. S. Afr. 15, 335–344.

Bieniawski, Z.T., 1989. Engineering Rock Mass Classifications: A Complete Manual for Engineers and Geologists in Mining, Civil, and Petroleum Engineering. John Wiley & Sons.

Garca-Sellés, D., Falivene, O., Arbués, P., Gratacos, O., Tavani, S., Muñoz, J.A., 2011. Supervised identification and reconstruction of near-planar geological surfaces from terrestrial laser scanning. Comput. Geosci. 37, 1584–1594.

Gigli, G., Casagli, N., 2011. Semi-automatic extraction of rock mass structural data from high resolution LiDAR point clouds. Int. J. Rock Mech. Min. Sci. 48, 187–198.

Haneberg, W.C., et al., 2007. Directional roughness profiles from three-dimensional photogrammetric or laser scanner point clouds. In: Eberhardt, E., Stead, D., Morrison, T. (Eds.), Rock Mechanics: Meeting Society's Challenges and Demands, pp. 101–106.

ISRM, 1977. The description of rock masses for engineering purposes: report by the Geological Society Engineering Group Working Party. Q. J. Eng. Geol. Hydrogeol. 10, 355–388.

Jaboyedoff, M., Metzger, R., Oppikofer, T., Couture, R., Derron, M.H., Locat, J., Turmel, D., 2007. New insight techniques to analyze rock-slope relief using DEM and 3D-imaging cloud points: Coltop-3D software. In: Francis, T. (Ed.), Rock Mechanics: Meeting Society's Challenges and Demands. Proceedings of the 1st Canada–U.S. Rock Mechanics Symposium, Vancouver, Canada, May 27–31, 2007, pp. 61–68.

Jaboyedoff, M., Oppikofer, T., Abellán, A., Derron, M.H., Loye, A., Metzger, R., Pedrazzini, A., 2012. Use of LiDAR in landslide investigations: a review. Nat. Hazards 61, 5–28.

Kemeny, J., Post, R., 2003. Estimating three-dimensional rock discontinuity orientation from digital images of fracture traces. Comput. Geosci. 29, 65–77 (URL: http://geol.queensu.ca/faculty/harrap/RockBench/downloads/files/2003%20-%20Kemeny.pdf).

Khoshelham, K., Altundag, D., Ngan-Tillard, D., Menenti, M., 2011. Influence of range measurement noise on roughness characterization of rock surfaces using terrestrial laser scanning. Int. J. Rock Mech. Min. Sci. 48, 1215–1223.

Lato, M.J., Vöge, M., 2012. Automated mapping of rock discontinuities in 3D LiDAR and photogrammetry models. Int. J. Rock Mech. Min. Sci. 54, 150–158.

MATLAB, 2013. Version 8.1.0.604 64 bit (win64) (R2013a). The MathWorks Inc., Natick, Massachusetts.

Olariu, M.I., Ferguson, J.F., Aiken, C.L., Xu, X., 2008. Outcrop fracture characterization using terrestrial laser scanners: deep-water Jackfork sandstone at Big Rock Quarry, Arkansas. Geosphere 4, 247–259.

Oppikofer, T., Jaboyedoff, M., Blikra, L., Derron, M.H., Metzger, R., 2009. Characterization and monitoring of the Åknes rockslide using terrestrial laser scanning. Nat. Hazards Earth Syst. Sci. 9, 1003–1019.

Oppikofer, T., Jaboyedoff, M., Pedrazzini, A., Derron, M.H., Blikra, L.H., 2011. Detailed DEM analysis of a rockslide scar to characterize the basal sliding surface of active rockslides. J. Geophys. Res. Earth Surf. 116. http://dx.doi.org/10.1029/2010JF001807 (n/a–n/a. doi: 10.1029/2010JF001807).

Palmstrom, A., 2001. Measurement and Characterization of Rock Mass Jointing. A.A. Balkema Publishers.

Piteau, D., 1970. Geological factors significant to the stability of slopes cut in rock. S. Afr. Inst. Min. Metall. 33–53.

Priest, S.D., 1993. Discontinuity Analysis for Rock Engineering. Springer.

Priest, S., Hudson, J., 1976. Discontinuity spacings in rock. International Journal of Rock Mechanics and Mining Sciences & Geomechanics Abstracts. Elsevier, pp. 135–148.

Riquelme, A.J., Abellán, A., Tomás, R., Jaboyedoff, M., 2014. A new approach for semi-automatic rock mass joints recognition from 3D point clouds. Comput. Geosci. 68, 38–52. http://dx.doi.org/10.1016/j.cageo.2014.03.014 (URL: http://www.sciencedirect.com/science/article/pii/S0098300414000740).

Silverman, B., 1986. Density Estimation for Statistics and Data Analysis. Chapman & Hall/CRC Monographs on Statistics & Applied Probability, Taylor & Francis (URL: http://books.google.es/books?id=e-xsrjsL7WkC).

Slob, S., 2010. Automated Rock Mass Characterisation Using 3-D Terrestrial Laser Scanning (Ph.D. thesis), TU Delft, Delft University of Technology (URL: http://www.narcis.nl/publication/RecordID/oai:tudelft.nl:uuid:c1481b1d-9b33-42e4-885a-53a6677843f6).

Slob, S., van Knapen, B., Hack, R., Turner, K., Kemeny, J., 2005. Method for automated discontinuity analysis of rock slopes with three-dimensional laser scanning. Transp. Res. Rec. 1913, 187–194.

Sturzenegger, M., Stead, D., 2009a. Close-range terrestrial digital photogrammetry and terrestrial laser scanning for discontinuity characterization on rock cuts. Eng. Geol. 106, 163–182. http://dx.doi.org/10.1016/j.enggeo.2009.03.004 (URL: http://www.sciencedirect.com/science/article/pii/S0013795209000556).

Sturzenegger, M., Stead, D., 2009b. Quantifying discontinuity orientation and persistence on high mountain rock slopes and large landslides using terrestrial remote sensing techniques. Nat. Hazards Earth Syst. Sci. 9, 267–287.

Sturzenegger, M., Stead, D., Elmo, D., 2011. Terrestrial remote sensing-based estimation of mean trace length, trace intensity and block size/shape. Eng. Geol. 119, 96–111.

Terzaghi, R.D., 1965. Sources of error in joint surveys. Geotechnique 15, 287–304.

Umili, G., Ferrero, A., Einstein, H., 2013. A new method for automatic discontinuity traces sampling on rock mass 3D model. Comput. Geosci. 51, 182–192. http://dx.doi.org/10.1016/j.cageo.2012.07.026 (URL: http://www.sciencedirect.com/science/article/pii/S0098300412002695).

Viero, A., Teza, G., Massironi, M., Jaboyedoff, M., Galgaro, A., 2010. Laser scanning-based recognition of rotational movements on a deep seated gravitational instability: the Cinque Torri case (north-eastern Italian Alps). Geomorphology 122, 191–204.